# Altered basal lipid metabolism underlies the functional impairment of naive CD8$^+$ T cells in elderly humans

**Short title:** Metabolic properties of naive CD8$^+$ T cells

Francesco Nicoli,[1,2,*] Mariela P. Cabral-Piccin,[1,10] Laura Papagno,[1,10] Eleonora Gallerani,[2] Victor Folcher,[1] Marion Dubois,[1] Emmanuel Clave,[3] Hélène Vallet,[1,4] Justin J. Frere,[5] Emma Gostick,[6] Sian Llewellyn-Lacey,[6] David A. Price,[6,7] Antoine Toubert,[3,8] Jacques Boddaert,[1,4] Antonella Caputo,[2] Riccardo Gavioli,[2] and Victor Appay[1,9,*]

[1] Centre d'Immunologie et des Maladies Infectieuses (CIMI-Paris), Sorbonne Université, INSERM U1135, 75013 Paris, France

[2] Department of Chemical and Pharmaceutical Sciences, University of Ferrara, Ferrara 44121, Italy

[4] Institut de Recherche Saint Louis, EMiLy, Université de Paris, INSERM U1160, 75010 Paris, France

[4] Service de Gériatrie, Hôpital Pitié-Salpêtrière, AP-HP, 75013 Paris, France

[5] Department of Immunobiology and the Arizona Center on Aging, University of Arizona College of Medicine Tucson, Tucson, AZ 85724, USA

[6] Division of Infection and Immunity, Cardiff University School of Medicine, Cardiff CF14 4XN, UK

[7] Systems Immunity Research Institute, Cardiff University School of Medicine, Cardiff CF14 4XN, UK

[8] Laboratoire d'Immunologie et d'Histocompatibilité, Hôpital Saint-Louis, AP-HP, 75010 Paris, France

[9] International Research Center of Medical Sciences, Kumamoto University, Kumamoto 860-0811, Japan

[10] These authors contributed equally

[*] Correspondence: nclfnc1@unife.it (F.N.) or victor.appay@upmc.fr (V.A.)

**ABSTRACT**

Aging is associated with functional deficits in the naive T cell compartment, which compromise the generation of *de novo* immune responses against previously unencountered antigens. The mechanisms that underlie this phenomenon have nonetheless remained unclear. We identified an age-related link between altered basal lipid metabolism and impaired antigen responsiveness in the naive $CD8^+$ T cell compartment. These abnormalities were associated with an enhanced susceptibility to activation-induced apoptosis and could be recapitulated *in vitro* by exposure to the homeostatic cytokine interleukin (IL)-7. Importantly, reversal of the bioenergetic anomalies with lipid-altering drugs, such as rosiglitazone, almost completely restored the functional capabilities of naive $CD8^+$ T cells. Interventions that favor lipid catabolism may therefore find utility as adjunctive therapies in the elderly to promote vaccine-induced immunity against emerging pathogens, such as seasonal influenza viruses and SARS-CoV-2.

**Keywords**

Fatty acids, immunometabolism, immunosenescence, naive T cells.

52 **INTRODUCTION**
53
54 Life expectancy has increased considerably over the last century as a consequence of advances in
55 medicine and improved public health systems. However, old age is associated with a high
56 prevalence of chronic diseases and an increased susceptibility to cancer and emerging pathogens,
57 such as SARS-CoV-2 (F. Nicoli et al., 2020). Age-related deficits in the immune system are
58 thought to play a key role in the development of many pathological conditions (Dorshkind &
59 Swain, 2009; Fulop et al., 2017; Ventura, Casciaro, Gangemi, & Buquicchio, 2017). Immune
60 aging is characterized by a progressive erosion of the naive $CD8^+$ T cell compartment, which
61 impairs *de novo* immune responses against newly encountered antigens (Briceno et al., 2016;
62 Nikolich-Zugich, 2014). In addition to a decline in absolute numbers (Wertheimer et al., 2014),
63 naive $CD8^+$ T cells in elderly individuals exhibit increased rates of homeostatic proliferation
64 (Sauce et al., 2012) and impaired differentiation in response to T cell receptor (TCR)-mediated
65 activation (Briceno et al., 2016).
66
67 A growing body of evidence indicates that lymphocyte metabolism is a key determinant of
68 immune functionality (Almeida, Lochner, Berod, & Sparwasser, 2016; Francesco Nicoli, 2020; F.
69 Nicoli, L. Papagno, et al., 2018; Palmer, Ostrowski, Balderson, Christian, & Crowe, 2015).
70 Systemic metabolic disturbances are common in elderly individuals, and increased levels of
71 adipokines and proinflammatory lipid species in particular have been implicated as critical
72 mediators of inflammaging, which is thought to exacerbate many age-related diseases (Baylis,
73 Bartlett, Patel, & Roberts, 2013). In this study, we investigated the bioenergetic features of naive
74 $CD8^+$ T cells in middle-aged and elderly humans, aiming to establish a link between metabolic
75 disturbances and immunosenescence. Naive $CD8^+$ T cells displayed a constellation of functional
76 and metabolic abnormalities in elderly people, including enhanced lipid influx and storage
77 accompanied by a marked susceptibility to apoptosis and impaired proliferation in response to

78 activation via the TCR. Importantly, these deficits were rectified in the presence of lipid-altering
79 drugs, opening potential therapeutic avenues to slow the process of immunosenescence.

80 **RESULTS**

81

82 **Naive CD8$^+$ T cells in the elderly are susceptible to apoptosis and exhibit impaired**
83 **proliferation after stimulation via the TCR**

84 In preliminary experiments, we compared the activation profiles of naive CD8$^+$ T cells in middle-
85 aged and elderly individuals, mimicking antigen-driven signals with plate-bound anti-CD3. No
86 age-related differences in activation per se were detected 24 hr after stimulation, as determined by
87 measuring the upregulation of CD69 and CD134 (Figure 1A). Signals transduced via the TCR
88 elicit an mTOR-driven metabolic switch that supports the function and the viability of activated
89 naive CD8$^+$ T cells (F. Nicoli, L. Papagno, et al., 2018). We therefore assessed mTOR activity in
90 parallel by quantifying phospho-S6 (pS6). In line with the comparable activation profiles, naive
91 CD8$^+$ T cells in middle-aged and elderly individuals upregulated mTOR activity to a similar
92 extent after stimulation with plate-bound anti-CD3 (Figure 1B).

93 To extend these findings, we measured the expression of metabolism-related genes, comparing
94 unstimulated and activated naive CD8$^+$ T cells (Figure 1C). Genes encoding various enzymes
95 involved in glycolysis were upregulated similarly in flow-sorted naive CD8$^+$ T cells from middle-
96 aged and elderly individuals after stimulation with plate-bound anti-CD3. In contrast, genes
97 associated with lipid metabolism or signaling pathways involved in metabolic regulation were not
98 generally upregulated in response to stimulation, with the exception of *MYC*, which was
99 overexpressed in activated naive CD8$^+$ T cells, irrespective of age. Genes that play a critical role
100 in the metabolic switch were also overexpressed in activated naive CD8$^+$ T cells, irrespective of
101 age, with the exception of *HIF1* and *RPS6KB1*, which were upregulated to a greater extent in
102 activated naive CD8$^+$ T cells from middle-aged *versus* elderly individuals.

103

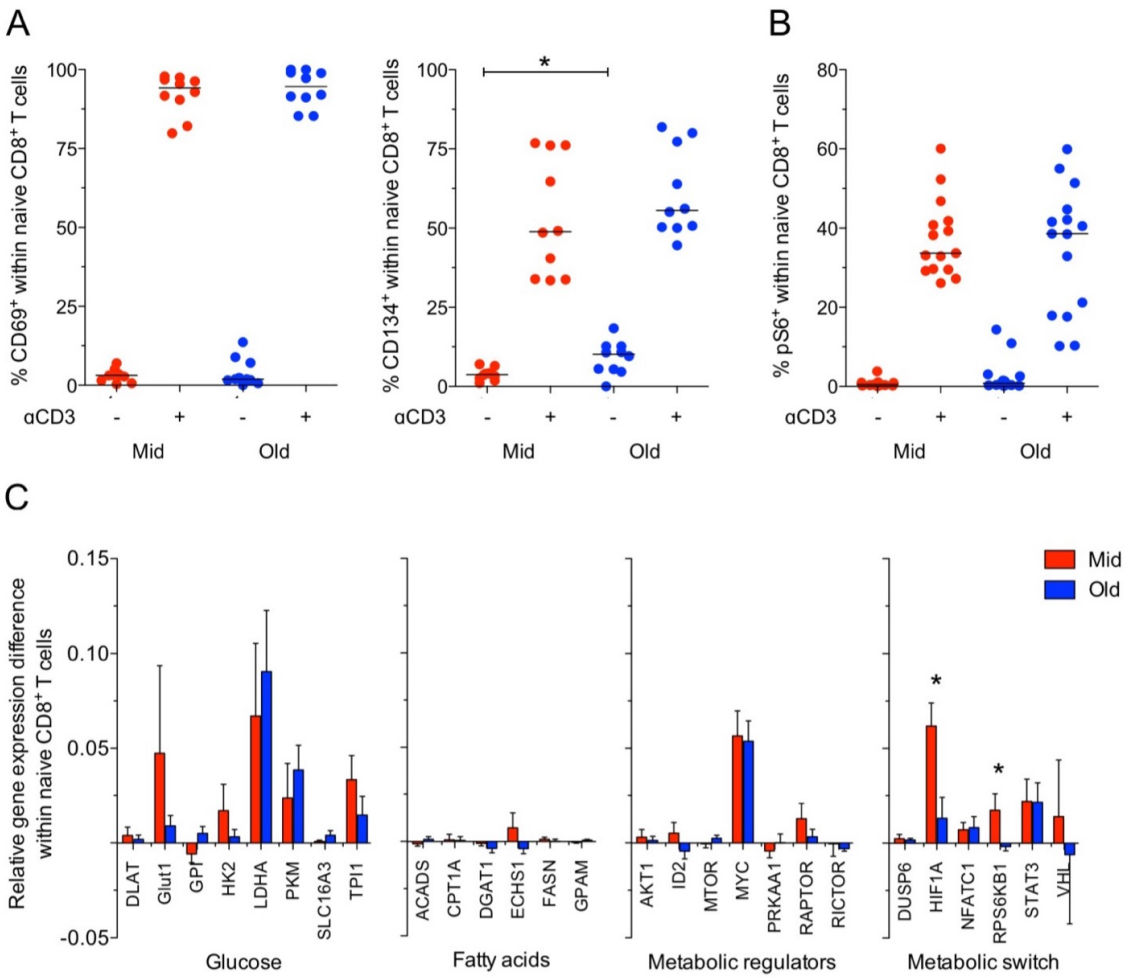


**Figure 1. Activation and gene expression in the naive CD8$^+$ T cell compartment.** (**A** & **B**) PBMCs from middle-aged (Mid) and elderly individuals (Old) were incubated in the absence or presence of plate-bound anti-CD3. Surface expression of the activation markers CD69 and CD134 was measured after 24 hr (A), and intracellular expression of mTOR activity marker pS6 was measured after 3 hr (B). Data are shown for naive CD8$^+$ T cells. Each dot represents one donor. Horizontal lines indicate median values. * $p < 0.05$ (Mann-Whitney *U* test). (**C**) Flow-sorted naive CD8$^+$ T cells from middle-aged (n = 4; Mid) and elderly individuals (n = 5; Old) were incubated in the absence or presence of plate-bound anti-CD3. Gene expression levels were measured after 3 hr. Data are shown relative to the unstimulated condition. Bars indicate mean ± SEM. * $p < 0.05$ (Mann-Whitney *U* test).

Despite these phenotypic and transcriptional similarities, naive CD8$^+$ T cells from middle-aged individuals proliferated to a greater extent than naive CD8$^+$ T cells from elderly individuals in response to stimulation with plate-bound anti-CD3 (Figure 2A), consistent with a previous report (Briceno et al., 2016). Early apoptosis was also less commonly observed among activated naive CD8$^+$ T cells from middle-aged *versus* elderly individuals, as determined by measuring the

121 expression of active caspase-3 (Figure 2B). In addition, we noted a strong inverse correlation
122 between the frequency of naive CD8$^+$ T cells that proliferated after stimulation and the frequency
123 of naive CD8$^+$ T cells that expressed active caspase-3 after stimulation, irrespective of age (Figure
124 2C).
125 Collectively, these data revealed that enhanced susceptibility to apoptosis was associated with an
126 age-related deficit in the proliferative capabilities of naive CD8$^+$ T cells, despite a largely
127 unaltered response to activation via the TCR.

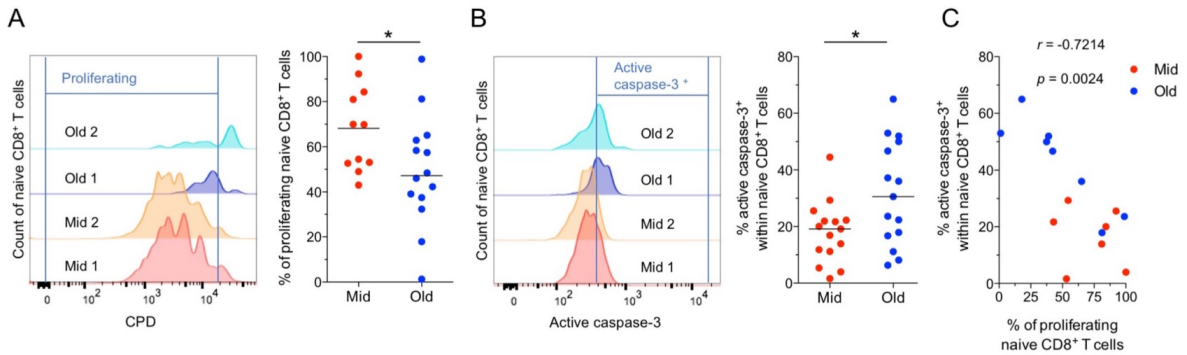


128

129 **Figure 2. Apoptosis and proliferation in the naive CD8$^+$ T cell compartment.** (**A** & **B**)
130 PBMCs from middle-aged (Mid) and elderly individuals (Old) were stimulated with plate-bound
131 anti-CD3. Proliferation was measured after 4 days (A), and active caspase-3 expression was
132 measured after 1 day (B). Left panels: representative flow cytometry profiles. Right panels: data
133 summaries. Data are shown for naive CD8$^+$ T cells. Each dot represents one donor. Horizontal
134 lines indicate median values. * $p < 0.05$ (Mann-Whitney U test). (**C**) Correlation between the
135 frequency of naive CD8$^+$ T cells that proliferated after stimulation and the frequency of naive
136 CD8$^+$ T cells that expressed active caspase-3 after stimulation. Each dot represents one donor.
137 Significance was determined using Spearman's rank correlation.
138

139

140 **Naive CD8$^+$ T cells in the elderly display elevated levels of basal activation**

141 Unstimulated naive CD8$^+$ T cells from middle-aged individuals expressed CD134 less commonly
142 than unstimulated naive CD8$^+$ T cells from elderly individuals (Figure 1A). To consolidate this
143 observation, which suggested increased levels of basal activation in the elderly, we measured the
144 expression of T-bet, which is classically upregulated in response to activation via the TCR. The
145 basal expression frequencies of T-bet mirrored the basal expression frequencies of CD134 (Figure

3A). Equivalent results were obtained using a more stringent definition of naive CD8$^+$ T cells (Figures S1A and S1B), which excluded phenotypically similar memory CD8$^+$ T cells (Pulko et al., 2016). The basal expression frequency of T-bet also correlated directly with the activation-induced expression frequency of active caspase-3 among naive CD8$^+$ T cells (Figure 3B).

Glycolysis is the main metabolic pathway that supports the activation of naive CD8$^+$ T cells (F. Nicoli, L. Papagno, et al., 2018; L. Zhang & Romero, 2018). We found no significant differences in basal glucose uptake between unstimulated naive CD8$^+$ T cells from middle-aged individuals and unstimulated naive CD8$^+$ T cells from elderly individuals (Figure 3C). Moreover, we found similar basal expression levels of glycolysis-related genes, with the exception of *HK2*, which was overexpressed in unstimulated naive CD8$^+$ T cells from middle-aged *versus* elderly individuals (Figure S2A). This gene encodes a selectively regulated isoform of hexokinase (H. Tan et al., 2017), which catalyzes glucose phosphorylation, and is usually induced in response to stimulation via the TCR (Lis et al., 2016; H. Tan et al., 2017).

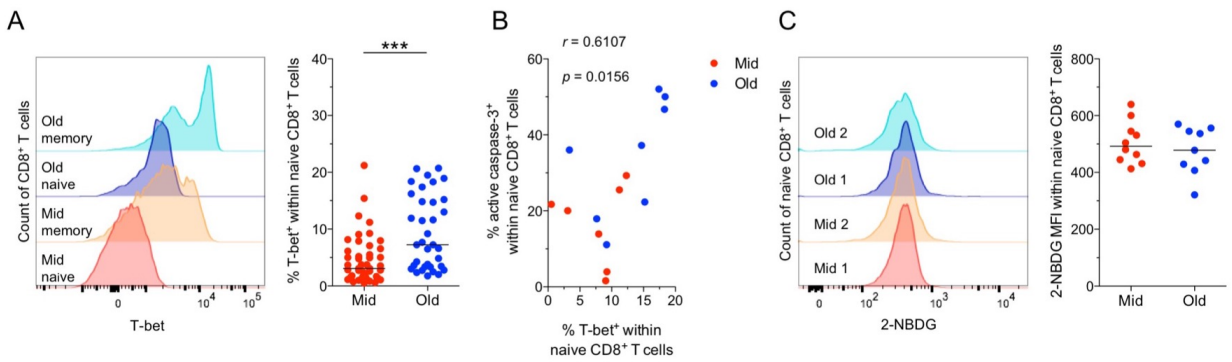


**Figure 3. Basal activation in the naive CD8$^+$ T cell compartment.** (**A**) T-bet expression was measured in unstimulated naive CD8$^+$ T cells from middle-aged (Mid) and elderly individuals (Old). Left panel: representative flow cytometry profiles. Right panel: data summary. Each dot represents one donor. Horizontal lines indicate median values. *** $p < 0.001$ (Mann-Whitney *U* test). (**B**) Correlation between the basal expression frequency of T-bet and the activation-induced expression frequency of active caspase-3 among naive CD8$^+$ T cells. Each dot represents one donor. Significance was determined using Spearman's rank correlation. (**C**) Glucose uptake was measured in unstimulated naive CD8$^+$ T cells from middle-aged (Mid) and elderly individuals (Old) by determining the mean fluorescence intensity (MFI) of 2-NBDG. Left panel: representative flow cytometry profiles. Right panel: data summary. Each dot represents one donor. Horizontal lines indicate median values. Significance was determined using the Mann-Whitney *U* test.

172 Collectively, these data revealed an age-related increase in the basal activation status of
173 unstimulated naive $CD8^+$ T cells, which appeared to be independent of the glycolysis pathway or
174 triggering via the TCR.
175
176
177 **Naive $CD8^+$ T cells in the elderly are metabolically distinct**
178 To explore these age-related homeostatic changes in more detail, we investigated the potential
179 roles of other metabolic pathways. Interestingly, fatty acid (FA) uptake was decreased among
180 unstimulated naive $CD8^+$ T cells from middle-aged *versus* elderly individuals (Figure 4A), but
181 this difference was not associated with significant changes in the expression levels of genes
182 encoding various enzymes involved in FA oxidation (FAO) or FA synthesis (FAS). However, we
183 noted that *DGAT1*, which encodes diacylglycerol O-acyltransferase 1, a key enzyme involved in
184 the storage of FAs as triacylglycerol (TAG), was expressed at lower levels in unstimulated naive
185 $CD8^+$ T cells from middle-aged *versus* elderly individuals (Figure S2B). In line with these results,
186 we also found that unstimulated naive $CD8^+$ T cells from middle-aged individuals stored lower
187 amounts of neutral lipids (NLs) than unstimulated naive $CD8^+$ T cells from elderly individuals
188 (Figure 4B).

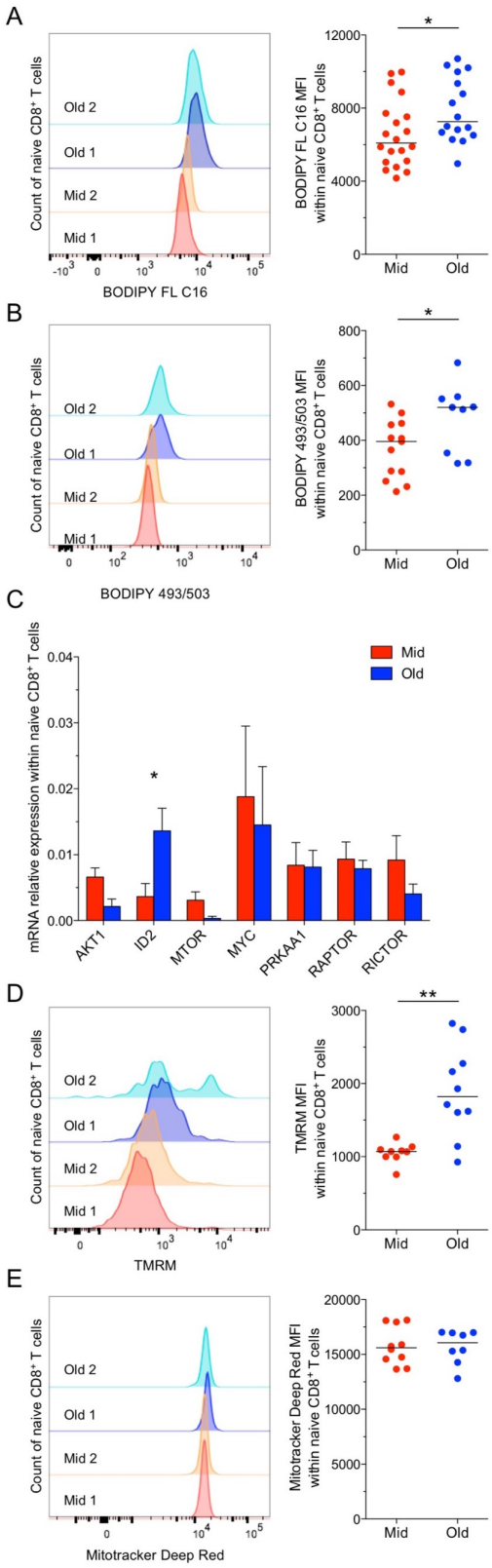


**Figure 4. Basal metabolism in the naive CD8$^+$ T cell compartment.** (**A** & **B**) FA uptake (A) and NL content (B) were measured in unstimulated naive CD8$^+$ T cells from middle-aged (Mid) and elderly individuals (Old) by determining the mean fluorescence intensity (MFI) of BODIPY FL C16 and BODIPY 493/503, respectively. Left panels: representative flow cytometry profiles.

194 Right panels: data summaries. Each dot represents one donor. Horizontal lines indicate median
195 values. * $p < 0.05$ (Mann-Whitney *U* test). (**C**) Expression levels of genes related to signaling
196 pathways involved in metabolic regulation were measured in unstimulated naive $CD8^+$ T cells
197 flow-sorted from middle-aged (n = 5; Mid) and elderly individuals (n = 5; Old). Data are shown
198 relative to the housekeeping gene 18S. Bars indicate mean ± SEM. * $p < 0.05$ (Mann-Whitney *U*
199 test). (**D** & **E**) Mitochondrial membrane potential (D) and mass (E) were measured in
200 unstimulated naive $CD8^+$ T cells from middle-aged (Mid) and elderly individuals (Old) by
201 determining the mean fluorescence intensity (MFI) of TMRM and Mitotracker Deep Red,
202 respectively. Left panels: representative flow cytometry profiles. Right panels: data summaries.
203 Each dot represents one donor. Horizontal lines indicate median values. ** $p < 0.01$ (Mann-
204 Whitney *U* test).
205

206 In further experiments, we assessed the basal expression levels of various genes encoding
207 transcription factors involved in metabolic regulation. Similar patterns of expression were
208 observed in unstimulated naive $CD8^+$ T cells, irrespective of age, with the exception of *ID2*,
209 which was expressed at lower levels in unstimulated naive $CD8^+$ T cells from middle-aged *versus*
210 elderly individuals (Figure 4C). *ID2* is involved in metabolic adaptation (Hou et al., 2009; Z.
211 Zhang, Rahme, Chatterjee, Havrda, & Israel, 2017) and promotes lipid storage via the
212 downmodulation of *PGC-1α* (Hou et al., 2009), which enhances FAO and inhibits TAG synthesis
213 (Morris et al., 2012). Moreover, *ID2* promotes an overall increase in mitochondrial membrane
214 potential (ΔΨM), without affecting mitochondrial biogenesis or, by extension, mitochondrial
215 mass (Z. Zhang et al., 2017). In line with these known functions, ΔΨM was lower in unstimulated
216 naive $CD8^+$ T cells from middle-aged *versus* elderly individuals (Figure 4D), whereas
217 mitochondrial mass was largely unaffected by age (Figure 4E). We also noted a direct correlation
218 between ΔΨM and the frequency of unstimulated naive $CD8^+$ T cells that expressed T-bet,
219 suggesting a link with the loss of quiescence (Figure S3).
220

221 Collectively, these data revealed an age-related shift in the basal metabolic properties of naive
222 $CD8^+$ T cells, typified by high levels of FA uptake and NL storage and a supranormal ΔΨM.
223

224 **Naive CD8$^+$ T cells in the elderly display high levels of lipid uptake and storage and**
225 **impaired priming in the presence of IL-7**

226 Naive CD8$^+$ T cells are maintained primarily via homeostatic proliferation in the elderly,
227 counteracting an age-related decrease in the rate of *de novo* production (Cicin-Sain et al., 2007;
228 Sauce et al., 2012). In turn, homeostatic proliferation is driven by the common cytokine receptor γ
229 chain family of cytokines, particularly interleukin (IL)-7 (Guimond, Fry, & Mackall, 2005),
230 which regulates the proliferation of naive and memory T cells under lymphopenic conditions (Fry
231 & Mackall, 2005; Surh & Sprent, 2005). We hypothesized that homeostatic proliferation might
232 alter the basal metabolic properties of naive CD8$^+$ T cells in elderly individuals, who typically
233 harbor increased plasma concentrations of IL-7 (Sauce et al., 2012). In line with this notion, we
234 found that *in vitro* treatment with IL-7 triggered FA uptake and NL storage in the naive CD8$^+$ T
235 cell compartment (Figure 5A and 5B).

236 To explore the biological relevance of this observation, we used an *in vitro* model to prime naive
237 CD8$^+$ T cells specific for the melanoma-associated epitope EV10 (Melan-A$_{26–35/A27L}$), which is
238 restricted by the common allotype HLA-A*02:01 (Gutjahr et al., 2019; F. Nicoli, L. Papagno, et
239 al., 2018). Pretreatment with IL-7 significantly inhibited the expansion of EV10-specific CD8$^+$ T
240 cells over a period of 10 days (Figure 5C). In contrast, no inhibition was observed if IL-7 was
241 added to the cultures on day 4 or day 7, after the initial encounter with cognate antigen (Fig.
242 S4A). Moreover, the addition of IL-7 on day 10 enhanced the recovery of EV10-specific CD8$^+$ T
243 cells on day 30, consistent with a survival effect in the memory compartment (Figure S4B).

244

245 Collectively, these data revealed an association between altered basal lipid metabolism and
246 impaired antigen responsiveness as a function of age in the naive CD8$^+$ T cell compartment, both
247 of which could be recapitulated with exogenous IL-7.

248

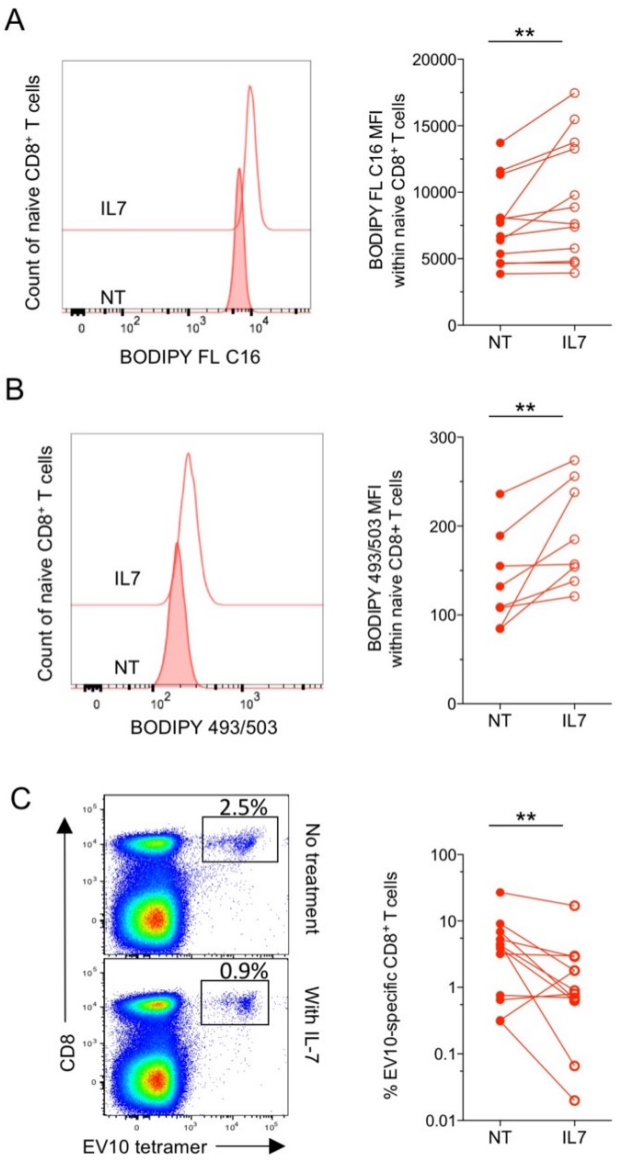


**Figure 5. Role of IL-7 in the naive CD8$^+$ T cell compartment.** (**A** & **B**) PBMCs from middle-aged individuals were incubated in the absence or presence of IL-7 for 24 (A) or 48 hr (B). FA uptake (A) and NL content (B) were measured in naive CD8$^+$ T cells by determining the mean fluorescence intensity (MFI) of BODIPY FL C16 and BODIPY 493/503, respectively. Left panels: representative flow cytometry profiles. Right panels: data summaries. Each dot represents one donor. ** $p < 0.01$ (Wilcoxon signed rank test). (**C**) Percentage of tetramer$^+$ EV10-specific CD8$^+$ T cells expanded for 10 days in the presence of Flt3 ligand and TLR8L after preincubation for 24 hr in the absence or presence of IL-7. Left panel: representative flow cytometry profiles. Right panel: data summary. Each dot represents one donor. ** $p < 0.01$ (Wilcoxon signed rank test). NT: not treated.

**Naive CD8$^+$ T cells in the elderly can be reinvigorated with lipid-altering drugs**

T cell homeostasis and viability can be affected by high levels of FAs (de Jong, Kloppenburg, Toes, & Ioan-Facsinay, 2014; Francesco Nicoli, Paul, & Appay, 2018). We therefore assessed the

potential link between apoptosis and lipid metabolism. The frequency of unstimulated naive CD8$^+$ T cells that expressed active caspase-3 correlated directly with basal levels of FA uptake (Figure 6A) and NL content (Figure 6B). To determine the biological relevance of these associations, we treated naive CD8$^+$ T cells with rosiglitazone, a drug known to foster lipid catabolism by activating triglyceride lipase (Kershaw et al., 2007) and preventing the conversion of FAs into NLs (Askari et al., 2007). Pretreatment with rosiglitazone inhibited activation-induced apoptosis among naive CD8$^+$ T cells, irrespective of age (Figure 6C). Similar results were obtained using fenofibrate, which induces lipid catabolism by enhancing FAO (Figure S5).

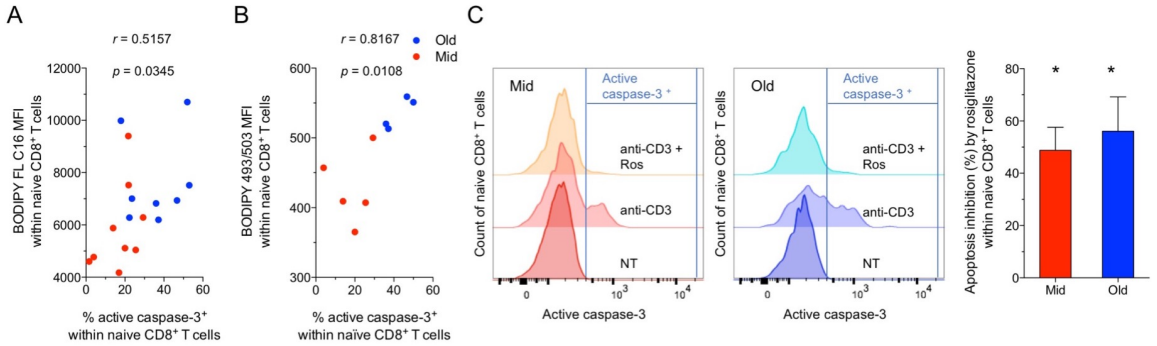


**Figure 6. Effects of lipid-altering drugs in the naive CD8$^+$ T cell compartment.** (**A** & **B**) Correlations between the frequency of unstimulated naive CD8$^+$ T cells that expressed active caspase-3 and basal levels of FA uptake (A) and NL content (B) measured by determining the mean fluorescence intensity (MFI) of BODIPY FL C16 and BODIPY 493/503, respectively. Each dot represents one donor. Significance was determined using Spearman's rank correlation. (**C**) PBMCs from middle-aged (n = 9; Mid) and elderly individuals (n = 8; Old) were stimulated with plate-bound anti-CD3 in the absence or presence of rosiglitazone (Ros). Active caspase-3 expression was measured after 24 hr. Data are shown for naive CD8$^+$ T cells. Left panel: representative flow cytometry profiles. Right panel: data summary. Bars indicate mean ± SEM. * $p < 0.05$ (Wilcoxon signed rank test).

In line with a previous study (Angela et al., 2016), we found that NLs accumulated in naive CD8$^+$ T cells as a function of proliferation in response to stimulation with plate-bound anti-CD3 (Figure 7A). We also found that proliferation under otherwise identical conditions was inhibited in the presence of hexadecyltrimethylammonium bromide (CTAB), which disrupts FA uptake (Figure 7B). This result was expected in light of the fact that FAs are essential components of cell

290 membranes. However, preincubation with palmitic acid, a common saturated FA, similarly
291 inhibited the proliferation of naive $CD8^+$ T cells in response to stimulation with plate-bound anti-
292 CD3 (Figure 7C). To explore these opposing effects in more detail, we tested our system using
293 two interventions, namely serum starvation, which inhibits FA uptake, and exposure to
294 rosiglitazone, which boosts NL catabolism (Figure 7D). Naive $CD8^+$ T cells from elderly
295 individuals proliferated to a greater extent after serum starvation, and the addition of rosiglitazone
296 further enhanced these activation-induced proliferative responses to levels approaching those
297 observed in direct comparisons with untreated naive $CD8^+$ T cells from middle-aged individuals
298 (Figure 7E). Of note, these interventions suppressed the activation-induced proliferation of naive
299 $CD8^+$ T cells from middle-aged individuals, highlighting the importance of basal activation and
300 lipid metabolism as determinants of therapeutic efficacy.
301
302 To assess the potential relevance of these findings in the context of antigen-driven immune
303 responses, we used our *in vitro* model to prime naive $CD8^+$ T cells specific for EV10 (Briceno et
304 al., 2016). As expected from the proliferation data, EV10-specific $CD8^+$ T cells from middle-aged
305 individuals expanded to a greater extent than EV10-specific $CD8^+$ T cells from elderly individuals
306 (Figure 7F), and preincubation with rosiglitazone consistently enhanced the expansion of EV10-
307 specific $CD8^+$ T cells from elderly individuals (Figure 7G),
308
309 Collectively, these data revealed that age-related functional deficits associated with abnormal
310 lipid metabolism and greater levels of basal activation in the naive $CD8^+$ T cell compartment were
311 reversed in the presence of rosiglitazone, offering a potentially useful therapeutic option to
312 enhance immune reactivity against newly encountered antigens in the elderly.
313

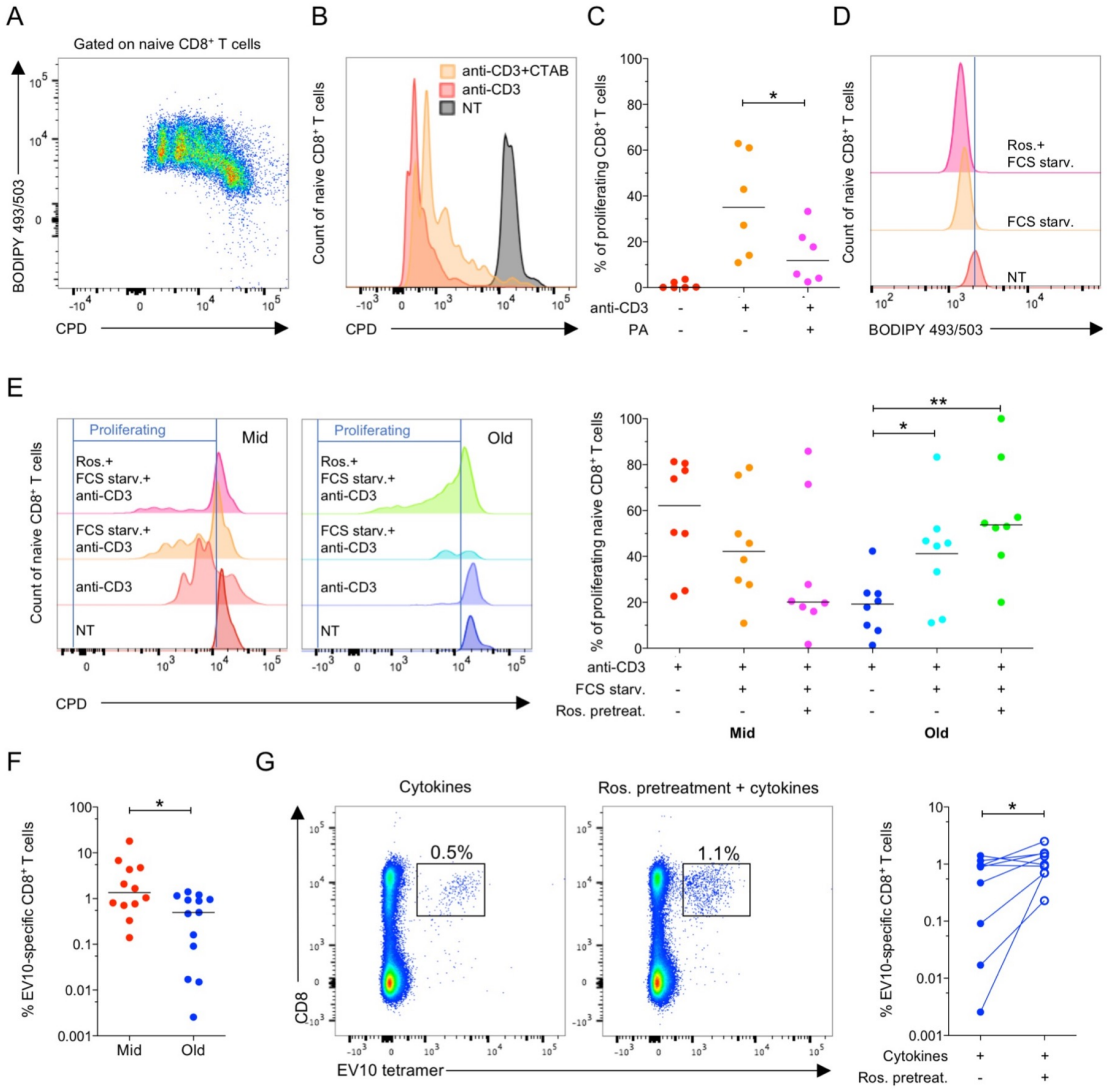


**Figure 7. Potential therapeutic properties of lipid-altering drugs in the naive CD8$^+$ T cell compartment.** (**A**–**C**) PBMCs from middle-aged individuals were stimulated with plate-bound anti-CD3. Proliferation was measured after 4 days. Data are shown for naive CD8$^+$ T cells. (A) NL content was measured by determining the mean fluorescence intensity (MFI) of BODIPY 493/503 and plotted against the dilution of Cell Proliferation Dye (CPD). Flow cytometry profiles are representative of three independent experiments. (B) PBMCs were stimulated in the absence or presence of hexadecyltrimethylammonium bromide (CTAB). Flow cytometry profiles are representative of three independent experiments. (C) PBMCs were preincubated for 1 day in serum-free medium in the absence or presence of palmitic acid (PA). Each dot represents one donor. Horizontal lines indicate median values. * $p < 0.05$ (Wilcoxon signed rank test). (**D**) PBMCs were preincubated for 2 days in serum-free medium in the absence or presence of rosiglitazone (Ros). NL content was measured in naive CD8$^+$ T cells by determining the mean fluorescence intensity (MFI) of BODIPY 493/503. Flow cytometry profiles are representative of five independent experiments. (**E**) PBMCs from middle-aged adults (Mid) and elderly individuals (Old) were preincubated for 2 days in serum-free medium in the absence or presence of rosiglitazone (Ros) and stimulated with plate-bound anti-CD3. Proliferation was measured after 4 days. Data are shown for naive CD8$^+$ T cells. Left panel: representative flow cytometry profiles. Right panel: data summary. Each dot represents one donor. Horizontal lines indicate median

333 values. * $p < 0.05$, ** $p < 0.01$ (Mann-Whitney *U* test). (**F**) Percentage of tetramer$^+$ EV10-specific
334 CD8$^+$ T cells expanded for 10 days in the presence of Flt3 ligand and a cocktail of inflammatory
335 cytokines. Each dot represents one donor. Horizontal lines indicate median values. * $p < 0.05$
336 (Mann-Whitney *U* test). (**G**) Percentage of tetramer$^+$ EV10-specific CD8$^+$ T cells expanded for 10
337 days in the presence of Flt3 ligand and a cocktail of inflammatory cytokines after preincubation
338 for 2 days in the absence or presence of rosiglitazone (Ros). Left panel: representative flow
339 cytometry profiles. Right panel: data summary. Each dot represents one donor. Horizontal lines
340 indicate median values. * $p < 0.05$ (Wilcoxon signed rank test). NT: not treated.
341

342 **DISCUSSION**

343 A detailed understanding of age-related deficits in the naive T cell compartment is essential for
344 the rational development of immunotherapies and vaccines that protect elderly individuals from
345 emerging threats, such as COVID-19. We found that naive CD8$^+$ T cells in elderly individuals
346 were susceptible to apoptosis and proliferated suboptimally in response to stimulation via the
347 TCR. These abnormalities were associated with enhanced levels of basal activation, measured in
348 terms of ΔΨM and the *ex vivo* expression frequencies of T-bet and CD134.

349

350 Recent studies have shown that metabolic processes govern the behavior of T cells (Gubser et al.,
351 2013; F. Nicoli, L. Papagno, et al., 2018; O'Neill, Kishton, & Rathmell, 2016; L. Zhang &
352 Romero, 2018). In the naive CD8$^+$ T cell compartment, autophagy and glycolysis are typically
353 upregulated in response to activation (Arnold et al., 2014; F. Nicoli, L. Papagno, et al., 2018;
354 Whang et al., 2017), whereas homeostatic energy requirements are fulfilled primarily via FAO
355 (Almeida et al., 2016; Green & Beck, 2017; O'Sullivan et al., 2014; Pearce et al., 2009; Raud,
356 McGuire, Jones, Sparwasser, & Berod, 2018). This metabolic switch was largely unaffected by
357 age in our study, but at rest, naive CD8$^+$ T cells in the elderly displayed abnormally high levels of
358 FA uptake and stored abnormally high amounts of NLs.

359

360 In line with previous reports showing that high levels of intracellular lipids may be toxic (de Jong
361 et al., 2014; F. Nicoli, L. Papagno, et al., 2018; Zurier, Rossetti, Seiler, & Laposata, 1999), we

362 found that active caspase-3 expression correlated directly with FA uptake and NL content in the
363 naive $CD8^+$ T cell compartment. Lipids are essential for T cell activation and proliferation
364 (Angela et al., 2016). Excessively high amounts of intracellular lipids can nonetheless impair T
365 cell proliferation and viability (Fernanda Cury-Boaventura, Cristine Kanunfre, Gorjao, Martins de
366 Lima, & Curi, 2006; Howie et al., 2017; Takahashi et al., 2012). Accordingly, we found that
367 activation-induced apoptosis was reduced by interventions that enhanced lipid clearance in naive
368 $CD8^+$ T cells. Of note, NLs *per se* are not toxic. The conversion of FAs into NLs therefore most
369 likely protects against lipotoxicity under homeostatic conditions (de Jong et al., 2014).
370
371 The heightened basal activation status of naive $CD8^+$ T cells in elderly individuals seemed to be
372 sustained energetically by increased mitochondrial activity, given that T-bet expression correlated
373 directly with $\Delta\Psi M$. Inflammation is closely linked with metabolic dysregulation in the elderly
374 (Pararasa et al., 2016). High levels of circulating proinflammatory cytokines and lipids are
375 common features of advanced age and may contribute to the disruption of cellular quiescence.
376 Moreover, hematopoietic progenitor cells in elderly individuals are often metabolically active,
377 and this characteristic may be heritable (Fali et al., 2018). Increased rates of homeostatic
378 proliferation are required to maintain naive $CD8^+$ T cell numbers in the elderly (Sauce et al.,
379 2012), and the predominant energetic pathway that supports this process is thought to be FAO
380 (Chang et al., 2013; Ibitokou et al., 2018). It is therefore plausible that high basal levels of FA
381 uptake and NL storage constitute a bioenergetic pattern that favors homeostatic proliferation. IL-7
382 is the main driver of homeostatic proliferation in this context (J. T. Tan et al., 2001), and plasma
383 levels of IL-7 are typically increased in the elderly (Sauce et al., 2012). We found that IL-7
384 promoted FA uptake and NL storage in the naive $CD8^+$ T cell compartment, as reported
385 previously for memory $CD8^+$ T cells (Cui et al., 2015). In line with the findings of this latter
386 study, IL-7 enhanced the *in vitro* survival of antigen-experienced $CD8^+$ T cells. However, IL-7

387 also inhibited the *in vitro* expansion of naive $CD8^+$ T cells in response to antigen encounter,
388 suggesting that homeostatic proliferation may compromise *de novo* adaptive immunity.
389
390 Aging is characterized by profound metabolic perturbations (Bonomini, Rodella, & Rezzani,
391 2015), including increased lipogenesis (Kuhla, Blei, Jaster, & Vollmar, 2011) and reduced
392 lipolysis (Toth & Tchernof, 2000), leading to higher systemic levels of free FAs and TAG (Mc
393 Auley & Mooney, 2015; Pararasa et al., 2016). The combination a homeostatic environment and
394 high systemic levels of proinflammatory cytokines and lipids may therefore underlie the altered
395 metabolism and functional deficits that characterize naive $CD8^+$ T cells in the elderly. A key
396 finding of our study was the observation that rosiglitazone, a drug already licensed for the
397 treatment of diabetes mellitus, can reverse these abnormalities. This is an encouraging result from
398 a translational perspective, akin to recent data showing that increased FAO can improve the
399 development and the quality of effector $CD8^+$ T cells (Chowdhury, Chamoto, & Honjo, 2018;
400 Chowdhury, Chamoto, Kumar, & Honjo, 2018; F. Nicoli, L. Papagno, et al., 2018; Y. Zhang et
401 al., 2017). Accordingly, we propose that lipid-altering drugs may be useful adjunctive therapies to
402 enhance adaptive immune responses against previously unencountered antigens, particularly in
403 elderly individuals, who often respond poorly to vaccination and remain vulnerable to emerging
404 pathogens, such as seasonal influenza viruses and SARS-CoV-2.
405
406

407 **MATERIAL AND METHODS**

408

409 **Human subjects and samples**

410 Two groups of healthy volunteers were enrolled in this study: (i) middle-aged Caucasians (19–55
411 years); and (ii) elderly Caucasians (>65 years). Individuals with malignancies, acute diseases, or
412 severe chronic diseases, such as atherosclerosis, congestive heart failure, poorly controlled
413 diabetes mellitus, renal or hepatic disease, various inflammatory conditions, or chronic
414 obstructive pulmonary disease, as well as individuals on immunosuppressive therapy, were
415 excluded from the study. Ethical approval was granted by the Comité de Protection des Personnes
416 of the Pitié Salpétrière Hospital (Paris, France). All volunteers provided written informed consent
417 in accordance with the Declaration of Helsinki. PBMCs were isolated from venous blood samples
418 via density gradient centrifugation according to standard protocols and cryopreserved in complete
419 medium supplemented with dimethyl sulfoxide (DMSO; 10% v/v; Sigma-Aldrich) and fetal calf
420 serum (FCS; 20% v/v; Sigma-Aldrich). Complete medium (R+) consisted of RPMI 1640
421 supplemented with non-essential amino acids (1% v/v), penicillin/streptomycin (100 U/mL), L-
422 glutamine (2 mM), and sodium pyruvate (1 mM) (all from Thermo Fisher Scientific).

423

424 **Flow cytometry and cell sorting**

425 PBMCs were stained for surface markers using combinations of the following directly conjugated
426 monoclonal antibodies: anti-CCR7–BV650 (clone 3D12; BD Biosciences), anti-CCR7–PE-Cy7
427 (clone 3D12; BD Biosciences), anti-CD3–BV605 (clone SK7; BD Biosciences), anti-CD8–APC
428 (clone RPA-T8; BD Biosciences), anti-CD8–APC-Cy7 (clone SK1; BD Biosciences), anti-CD8–
429 FITC (clone RPA-T8; BD Biosciences), anti-CD27–AF700 (clone O323; BioLegend), anti-
430 CD27–PE (clone M-T271; BD Biosciences), anti-CD45RA–ECD (clone 2H4LDH11LDB9;
431 Beckman Coulter), anti-CD45RA–PerCP-Cy5.5 (clone HI100; eBioscience), anti-CD45RA–V450

432 (clone HI100; BD Biosciences), anti-CD49b–PE-Cy7 (clone 9F10; BioLegend), anti-CD57–
433 Pacific Blue (clone HCD57; BioLegend), and anti-CD95–FITC (clone DX2; BD Biosciences).
434 Naive $CD8^+$ T cells were defined as $CD3^+$ $CD8^+$ $CD27^+$ $CD45RA^+$ $CCR7^+$ in most experiments
435 and further identified as $CD49b^-$ $CD57^-$ $CD95^-$ for gene expression studies and intracellular
436 measurements of T-bet. Non-viable cells were eliminated from the analysis using LIVE/DEAD
437 Fixable Aqua (Thermo Fisher Scientific). Intracellular stains were performed using anti-T-bet–
438 eFluor660 (clone 4B10; eBioscience) in conjunction with a Transcription Factor Buffer Set (BD
439 Biosciences). Samples were acquired using an LSR Fortessa or a FACSCanto II (BD
440 Biosciences). Naive $CD8^+$ T-cells were flow-sorted using a FACSAria II (BD Biosciences). Data
441 were analyzed using FACSDiva software version 7 (BD Biosciences) and/or FlowJo software
442 version 10 (FlowJo LLC).
443
444 **Activation and apoptosis assays**
445 PBMCs were stimulated for 24 hr with plate-bound anti-CD3 (clone OKT3; Thermo Fisher
446 Scientific) in the absence or presence of fenofibrate (50 μM; Sigma-Aldrich) or rosiglitazone (40
447 μM; Sigma-Aldrich). Activation markers were quantified on the cell surface using anti-CD69–
448 FITC (clone L78; BD Biosciences) and anti-CD134–BV711 (clone ACT35; BD Biosciences).
449 Intracellular stains were performed using anti-active caspase-3–PE (clone C92-605; BD
450 Biosciences) in conjunction with a Cytofix/Cytoperm Fixation/Permeabilization Solution Kit (BD
451 Biosciences).
452
453 **Metabolism assays**
454 To determine glucose uptake, PBMCs were incubated in phosphate-buffered saline (PBS)
455 containing 2′-(N-(7-nitrobenz-2-oxa-1,3-diazol-4-yl)amino)-2-deoxyglucose (2-NBDG; 50 μM;
456 Thermo Fisher Scientific). To determine FA uptake, PBMCs were incubated for 20 min at 37°C

457 in PBS containing 4,4-difluoro-5,7-dimethyl-4-bora-3a,4a-diaza-*s*-indacene-3-hexadecanoic acid
458 (BODIPY FL C16; 1 μM; Thermo Fisher Scientific). To determine neutral lipid content, PBMCs
459 were incubated for 20 min at 37°C in PBS containing 4,4-difluoro-1,3,5,7,8-pentamethyl-4-bora-
460 3a,4a-diaza-*s*-indacene (BODIPY 493/503; 10 μM; Thermo Fisher Scientific). To determine
461 mitochondrial mass, PBMCs were incubated for 30 min at 37°C in R+ containing Mitotracker
462 Deep Red (500 nM; Thermo Fisher Scientific). To determine mitochondrial membrane potential,
463 PBMCs were incubated for 30 min at 37°C in R+ containing tetramethylrhodamine, methyl ester,
464 perchlorate (TMRM; 25 nM; Thermo Fisher Scientific). To determine mTOR activity, PBMCs
465 were incubated for 10 min at 37°C in Cytofix Fixation Buffer (BD Biosciences), washed,
466 incubated for 30 min at 4°C in Phosflow Perm Buffer III (BD Biosciences), washed again, and
467 stained for 1 hr at room temperature with anti-pS6–Pacific Blue (clone D57.2.2E; Cell Signaling
468 Technology).
469
470 **Proliferation assays**
471 PBMCs were labeled with Cell Proliferation Dye (CPD) eFluor450 (Thermo Fisher Scientific)
472 and stimulated for 4 days with plate-bound anti-CD3 (clone OKT3; Thermo Fisher Scientific) in
473 the absence or presence of CTAB (1 μM; Sigma-Aldrich). In some experiments, cells were
474 precultured in AIM-V medium (Thermo Fisher Scientific) supplemented with bovine serum
475 albumin (BSA; 10% v/v; Sigma-Aldrich) for 1 day in the absence or presence of palmitic acid
476 (300 μM; Sigma-Aldrich), and in other experiments, cells were precultured in AIM-V medium
477 (Thermo Fisher Scientific) without BSA supplementation for 2 days in the absence or presence of
478 rosiglitazone (40 μM; Sigma-Aldrich). Proliferation was measured using flow cytometry to
479 quantify the dilution of CPD.
480
481 **Peptides and tetramers**

482 All peptides were synthesized at >95% purity (BioSynthesis Inc.). The EV20 peptide
483 (YTAAEELAGIGILTVILGVL, Melan-$A_{21–40/A27L}$) was used for *in vitro* priming studies.
484 Fluorochrome-labeled tetrameric complexes of HLA-A*02:01–EV10 (ELAGIGILTV, Melan-
485 $A_{26–35/A27L}$) were generated in-house as described previously (Price et al., 2005).
486

487 ***In vitro* priming of antigen-specific CD8$^+$ T cells**

488 Naive precursors specific for HLA-A2–EV10 were primed *in vitro* using an accelerated dendritic
489 cell (DC) coculture protocol as described previously (Alanio et al., 2015; Lissina et al., 2016; F.
490 Nicoli, L. Papagno, et al., 2018). Briefly, thawed PBMCs were resuspended at $5 \times 10^6$ cells/well
491 in AIM-V medium (Thermo Fisher Scientific) supplemented with Flt3 ligand (Flt3L; 50 ng/ml;
492 R&D Systems) in the absence or presence of rosiglitazone (40 μM; Sigma-Aldrich) or IL-7 (20
493 ng/mL; R&D Systems). After 24 hr (day 1), the Melan-A peptide EV20 (1 μM) was added to the
494 cultures, and DC maturation was induced using a standard cocktail of inflammatory cytokines,
495 incorporating IL-1β (10 ng/mL), IL-7 (0.5 ng/mL), prostaglandin E2 (PGE2; 1 μM), and TNF
496 (1,000 U/mL) (all from R&D Systems), or ssRNA40 (TLR8L; 0.5 μg/mL; InvivoGen). The
497 cultures were supplemented on day 2 with FCS (10% v/v; Sigma-Aldrich). Medium was replaced
498 every 3 days thereafter with fresh R+ containing FCS (10% v/v; Sigma-Aldrich). In some
499 experiments, the cultures were further supplemented on day 4 or day 7 with IL-7 (10 ng/mL;
500 R&D Systems). Antigen-specific CD8$^+$ T cells were characterized via flow cytometry on day 10.
501 Long-term cultures were maintained similarly until day 30 in the absence or presence of IL-7 (10
502 mg/mL; R&D Systems).
503

504 **RNA extraction and qPCR analysis**

505 PBMCs were activated for 5 hr with plate-bound anti-CD3 (clone OKT3; Thermo Fisher
506 Scientific). RNA was extracted from flow-sorted naive CD8$^+$ T cells (n = 300 per condition)

using a NucleoSpin RNA XS Kit (Macherey-Nagel), and cDNA was synthesized using Reverse Transcription Master Mix (Fluidigm). Specific targets were amplified using PreAmp Master Mix (Fluidigm). Gene expression was assessed using a BioMark HD System (Fluidigm) with EvaGreen Supermix (Bio-Rad). RNA expression levels were calculated using the $2^{-\Delta\Delta CT}$ method with reference to a housekeeping gene (human 18S) (F. Nicoli, E. Gallerani, et al., 2018).

**General statistics**

Univariate statistical analyses were performed using nonparametric tests in Prism software version 8 (GraphPad Software Inc.). Significance was assigned at $p < 0.05$.

**ACKNOWLEDGEMENTS**

We thank Simone Candioli and Silvio Spatocco (University of Ferrara, Italy), Irene Bonazzi and Ilaria Signoretto (University of Padua, Italy), and Alain Savenay (AP-HP, Paris, France) for technical assistance, Mario Pende (Institut Necker-Enfants Malades, Paris, France) for helpful discussions, and Veronique Morin and Rima Zoorob (INSERM U1135, Paris, France) and Silvia Menegatti and Lars Rogge (Institut Pasteur, Paris, France) for assistance with gene expression analyses. This work was supported by the Agence National de la Recherche (ANR-14-CE14-0030-01) and the Université Franco-Italienne/Università Italo-Francese (Galileo Project G10-718; PHC Galilee Project 39582TJ). Core provision of the FACSCanto II was funded by the University of Ferrara (Bando per l'acquisizione di strumenti per la ricerca di ateneo-2015). D.A.P. was supported by a Wellcome Trust Senior Investigator Award (100326/Z/12/Z).

**CONFLICT OF INTERESTS**

The authors declare no conflict of interest.

**AUTHORS' CONTRIBUTIONS**

F.N., R.G., and V.A. conceptualized the project; F.N., M.P.C.P., L.P., E.Ga., V.F., and J.J.F. performed experiments and analyzed data; M.D., E.C., H.V., E.Go., S.L.L., D.A.P., A.T., and J.B. provided critical resources; F.N., J.F.F., R.G., and V.A. drafted the manuscript; F.N., D.A.P., A.C., R.G., and V.A. edited the manuscript; D.A.P., A.T., A.C., and V.A. acquired funds to support the work. All authors contributed intellectually and approved the manuscript.

546 **REFERENCES**

547

548 Alanio, C., Nicoli, F., Sultanik, P., Flecken, T., Perot, B., Duffy, D., . . . Albert, M. L. (2015).
549 Bystander hyperactivation of preimmune CD8+ T cells in chronic HCV patients. *Elife, 4*, 1-
550 20. doi:10.7554/eLife.07916
551 Almeida, L., Lochner, M., Berod, L., & Sparwasser, T. (2016). Metabolic pathways in T cell
552 activation and lineage differentiation. *Semin Immunol, 28*(5), 514-524.
553 doi:10.1016/j.smim.2016.10.009
554 Angela, M., Endo, Y., Asou, H. K., Yamamoto, T., Tumes, D. J., Tokuyama, H., . . . Nakayama, T.
555 (2016). Fatty acid metabolic reprogramming via mTOR-mediated inductions of
556 PPARgamma directs early activation of T cells. *Nat Commun, 7*, 13683.
557 doi:10.1038/ncomms13683
558 Arnold, C. R., Pritz, T., Brunner, S., Knabb, C., Salvenmoser, W., Holzwarth, B., . . . Grubeck-
559 Loebenstein, B. (2014). T cell receptor-mediated activation is a potent inducer of
560 macroautophagy in human CD8(+)CD28(+) T cells but not in CD8(+)CD28(-) T cells. *Exp*
561 *Gerontol, 54*, 75-83. doi:10.1016/j.exger.2014.01.018
562 Askari, B., Kanter, J. E., Sherrid, A. M., Golej, D. L., Bender, A. T., Liu, J., . . . Bornfeldt, K. E. (2007).
563 Rosiglitazone inhibits acyl-CoA synthetase activity and fatty acid partitioning to
564 diacylglycerol and triacylglycerol via a peroxisome proliferator-activated receptor-
565 gamma-independent mechanism in human arterial smooth muscle cells and
566 macrophages. *Diabetes, 56*(4), 1143-1152. doi:10.2337/db06-0267
567 Baylis, D., Bartlett, D. B., Patel, H. P., & Roberts, H. C. (2013). Understanding how we age:
568 insights into inflammaging. *Longev Healthspan, 2*(1), 8. doi:10.1186/2046-2395-2-8
569 Bonomini, F., Rodella, L. F., & Rezzani, R. (2015). Metabolic syndrome, aging and involvement of
570 oxidative stress. *Aging Dis, 6*(2), 109-120. doi:10.14336/AD.2014.0305
571 Briceno, O., Lissina, A., Wanke, K., Afonso, G., von Braun, A., Ragon, K., . . . Appay, V. (2016).
572 Reduced naive CD8(+) T-cell priming efficacy in elderly adults. *Aging Cell, 15*(1), 14-21.
573 doi:10.1111/acel.12384
574 Chang, C. H., Curtis, J. D., Maggi, L. B., Jr., Faubert, B., Villarino, A. V., O'Sullivan, D., . . . Pearce, E.
575 L. (2013). Posttranscriptional control of T cell effector function by aerobic glycolysis. *Cell,*
576 *153*(6), 1239-1251. doi:10.1016/j.cell.2013.05.016
577 Chowdhury, P. S., Chamoto, K., & Honjo, T. (2018). Combination therapy strategies for improving
578 PD-1 blockade efficacy: a new era in cancer immunotherapy. *J Intern Med, 283*(2), 110-
579 120. doi:10.1111/joim.12708
580 Chowdhury, P. S., Chamoto, K., Kumar, A., & Honjo, T. (2018). PPAR-Induced Fatty Acid Oxidation
581 in T Cells Increases the Number of Tumor-Reactive CD8(+) T Cells and Facilitates Anti-PD-
582 1 Therapy. *Cancer Immunol Res*. doi:10.1158/2326-6066.CIR-18-0095
583 Cicin-Sain, L., Messaoudi, I., Park, B., Currier, N., Planer, S., Fischer, M., . . . Nikolich-Zugich, J.
584 (2007). Dramatic increase in naive T cell turnover is linked to loss of naive T cells from old
585 primates. *Proc Natl Acad Sci U S A, 104*(50), 19960-19965. doi:10.1073/pnas.0705905104
586 Cui, G., Staron, M. M., Gray, S. M., Ho, P. C., Amezquita, R. A., Wu, J., & Kaech, S. M. (2015). IL-7-
587 Induced Glycerol Transport and TAG Synthesis Promotes Memory CD8+ T Cell Longevity.
588 *Cell, 161*(4), 750-761. doi:10.1016/j.cell.2015.03.021
589 de Jong, A. J., Kloppenburg, M., Toes, R. E., & Ioan-Facsinay, A. (2014). Fatty acids, lipid
590 mediators, and T-cell function. *Front Immunol, 5*, 483. doi:10.3389/fimmu.2014.00483

591 Dorshkind, K., & Swain, S. (2009). Age-associated declines in immune system development and
592 function: causes, consequences, and reversal. *Curr Opin Immunol, 21*(4), 404-407.
593 doi:10.1016/j.coi.2009.07.001
594 Fali, T., Fabre-Mersseman, V., Yamamoto, T., Bayard, C., Papagno, L., Fastenackels, S., . . . Appay,
595 V. (2018). Elderly human hematopoietic progenitor cells express cellular senescence
596 markers and are more susceptible to pyroptosis. *JCI Insight, 3*(13).
597 doi:10.1172/jci.insight.95319
598 Fernanda Cury-Boaventura, M., Cristine Kanunfre, C., Gorjao, R., Martins de Lima, T., & Curi, R.
599 (2006). Mechanisms involved in Jurkat cell death induced by oleic and linoleic acids. *Clin*
600 *Nutr, 25*(6), 1004-1014. doi:10.1016/j.clnu.2006.05.008
601 Fry, T. J., & Mackall, C. L. (2005). The many faces of IL-7: from lymphopoiesis to peripheral T cell
602 maintenance. *J Immunol, 174*(11), 6571-6576.
603 Fulop, T., Larbi, A., Dupuis, G., Le Page, A., Frost, E. H., Cohen, A. A., . . . Franceschi, C. (2017).
604 Immunosenescence and Inflamm-Aging As Two Sides of the Same Coin: Friends or Foes?
605 *Front Immunol, 8*, 1960. doi:10.3389/fimmu.2017.01960
606 Green, W. D., & Beck, M. A. (2017). Obesity altered T cell metabolism and the response to
607 infection. *Curr Opin Immunol, 46*, 1-7. doi:10.1016/j.coi.2017.03.008
608 Gubser, P. M., Bantug, G. R., Razik, L., Fischer, M., Dimeloe, S., Hoenger, G., . . . Hess, C. (2013).
609 Rapid effector function of memory CD8+ T cells requires an immediate-early glycolytic
610 switch. *Nat Immunol, 14*(10), 1064-1072. doi:10.1038/ni.2687
611 Guimond, M., Fry, T. J., & Mackall, C. L. (2005). Cytokine signals in T-cell homeostasis. *J*
612 *Immunother, 28*(4), 289-294.
613 Gutjahr, A., Papagno, L., Nicoli, F., Kanuma, T., Kuse, N., Cabral-Piccin, M. P., . . . Appay, V.
614 (2019). The STING ligand cGAMP potentiates the efficacy of vaccine-induced CD8+ T cells.
615 *JCI Insight, 4*(7). doi:10.1172/jci.insight.125107
616 Hou, T. Y., Ward, S. M., Murad, J. M., Watson, N. P., Israel, M. A., & Duffield, G. E. (2009). ID2
617 (inhibitor of DNA binding 2) is a rhythmically expressed transcriptional repressor required
618 for circadian clock output in mouse liver. *J Biol Chem, 284*(46), 31735-31745.
619 doi:10.1074/jbc.M109.013961
620 Howie, D., Cobbold, S. P., Adams, E., Ten Bokum, A., Necula, A. S., Zhang, W., . . . Waldmann, H.
621 (2017). Foxp3 drives oxidative phosphorylation and protection from lipotoxicity. *JCI*
622 *Insight, 2*(3), e89160. doi:10.1172/jci.insight.89160
623 Ibitokou, S. A., Dillon, B. E., Sinha, M., Szczesny, B., Delgadillo, A., Reda Abdelrahman, D., . . .
624 Stephens, R. (2018). Early Inhibition of Fatty Acid Synthesis Reduces Generation of
625 Memory Precursor Effector T Cells in Chronic Infection. *J Immunol, 200*(2), 643-656.
626 doi:10.4049/jimmunol.1602110
627 Kershaw, E. E., Schupp, M., Guan, H. P., Gardner, N. P., Lazar, M. A., & Flier, J. S. (2007).
628 PPARgamma regulates adipose triglyceride lipase in adipocytes in vitro and in vivo. *Am J*
629 *Physiol Endocrinol Metab, 293*(6), E1736-1745. doi:10.1152/ajpendo.00122.2007
630 Kuhla, A., Blei, T., Jaster, R., & Vollmar, B. (2011). Aging is associated with a shift of fatty
631 metabolism toward lipogenesis. *J Gerontol A Biol Sci Med Sci, 66*(11), 1192-1200.
632 doi:10.1093/gerona/glr124
633 Lis, P., Dylag, M., Niedzwiecka, K., Ko, Y. H., Pedersen, P. L., Goffeau, A., & Ulaszewski, S. (2016).
634 The HK2 Dependent "Warburg Effect" and Mitochondrial Oxidative Phosphorylation in
635 Cancer: Targets for Effective Therapy with 3-Bromopyruvate. *Molecules, 21*(12).
636 doi:10.3390/molecules21121730

637 Lissina, A., Briceno, O., Afonso, G., Larsen, M., Gostick, E., Price, D. A., . . . Appay, V. (2016).
638 Priming of Qualitatively Superior Human Effector CD8+ T Cells Using TLR8 Ligand
639 Combined with FLT3 Ligand. *J Immunol, 196*(1), 256-263. doi:10.4049/jimmunol.1501140
640 Mc Auley, M. T., & Mooney, K. M. (2015). Computationally Modeling Lipid Metabolism and
641 Aging: A Mini-review. *Comput Struct Biotechnol J, 13*, 38-46.
642 doi:10.1016/j.csbj.2014.11.006
643 Morris, E. M., Meers, G. M., Booth, F. W., Fritsche, K. L., Hardin, C. D., Thyfault, J. P., & Ibdah, J.
644 A. (2012). PGC-1alpha overexpression results in increased hepatic fatty acid oxidation
645 with reduced triacylglycerol accumulation and secretion. *Am J Physiol Gastrointest Liver*
646 *Physiol, 303*(8), G979-992. doi:10.1152/ajpgi.00169.2012
647 Nicoli, F. (2020). Angry, Hungry T-Cells: How Are T-Cell Responses Induced in Low Nutrient
648 Conditions? *Immunometabolism, 2*(1), e200004. doi:10.20900/immunometab20200004
649 Nicoli, F., Gallerani, E., Sforza, F., Finessi, V., Chachage, M., Geldmacher, C., . . . Gavioli, R. (2018).
650 The HIV-1 Tat protein affects human CD4+ T-cell programing and activation, and favors
651 the differentiation of naive CD4+ T cells. *AIDS, 32*(5), 575-581.
652 doi:10.1097/QAD.0000000000001734
653 Nicoli, F., Papagno, L., Frere, J. J., Cabral-Piccin, M. P., Clave, E., Gostick, E., . . . Appay, V. (2018).
654 Naive CD8(+) T-Cells Engage a Versatile Metabolic Program Upon Activation in Humans
655 and Differ Energetically From Memory CD8(+) T-Cells. *Front Immunol, 9*, 2736.
656 doi:10.3389/fimmu.2018.02736
657 Nicoli, F., Paul, S., & Appay, V. (2018). Harnessing the Induction of CD8+ T-Cell Responses
658 Through Metabolic Regulation by Pathogen-Recognition-Receptor Triggering in Antigen
659 Presenting Cells. *Frontiers in Immunology, 9*(2372). doi:10.3389/fimmu.2018.02372
660 Nicoli, F., Solis-Soto, M. T., Paudel, D., Marconi, P., Gavioli, R., Appay, V., & Caputo, A. (2020).
661 Age-related decline of de novo T cell responsiveness as a cause of COVID-19 severity.
662 *Geroscience*. doi:10.1007/s11357-020-00217-w
663 Nikolich-Zugich, J. (2014). Aging of the T cell compartment in mice and humans: from no naive
664 expectations to foggy memories. *J Immunol, 193*(6), 2622-2629.
665 doi:10.4049/jimmunol.1401174
666 O'Neill, L. A., Kishton, R. J., & Rathmell, J. (2016). A guide to immunometabolism for
667 immunologists. *Nat Rev Immunol, 16*(9), 553-565. doi:10.1038/nri.2016.70
668 O'Sullivan, D., van der Windt, G. J., Huang, S. C., Curtis, J. D., Chang, C. H., Buck, M. D., . . .
669 Pearce, E. L. (2014). Memory CD8(+) T cells use cell-intrinsic lipolysis to support the
670 metabolic programming necessary for development. *Immunity, 41*(1), 75-88.
671 doi:10.1016/j.immuni.2014.06.005
672 Palmer, C. S., Ostrowski, M., Balderson, B., Christian, N., & Crowe, S. M. (2015). Glucose
673 metabolism regulates T cell activation, differentiation, and functions. *Front Immunol, 6*,
674 1. doi:10.3389/fimmu.2015.00001
675 Pararasa, C., Ikwuobe, J., Shigdar, S., Boukouvalas, A., Nabney, I. T., Brown, J. E., . . . Griffiths, H.
676 R. (2016). Age-associated changes in long-chain fatty acid profile during healthy aging
677 promote pro-inflammatory monocyte polarization via PPARgamma. *Aging Cell, 15*(1),
678 128-139. doi:10.1111/acel.12416
679 Pearce, E. L., Walsh, M. C., Cejas, P. J., Harms, G. M., Shen, H., Wang, L. S., . . . Choi, Y. (2009).
680 Enhancing CD8 T-cell memory by modulating fatty acid metabolism. *Nature, 460*(7251),
681 103-107. doi:10.1038/nature08097

682 Price, D. A., Brenchley, J. M., Ruff, L. E., Betts, M. R., Hill, B. J., Roederer, M., . . . Douek, D. C.
683 (2005). Avidity for antigen shapes clonal dominance in CD8+ T cell populations specific
684 for persistent DNA viruses. *J Exp Med, 202*(10), 1349-1361. doi:10.1084/jem.20051357
685 Pulko, V., Davies, J. S., Martinez, C., Lanteri, M. C., Busch, M. P., Diamond, M. S., . . . Nikolich-
686 Zugich, J. (2016). Human memory T cells with a naive phenotype accumulate with aging
687 and respond to persistent viruses. *Nat Immunol, 17*(8), 966-975. doi:10.1038/ni.3483
688 Raud, B., McGuire, P. J., Jones, R. G., Sparwasser, T., & Berod, L. (2018). Fatty acid metabolism in
689 CD8(+) T cell memory: Challenging current concepts. *Immunol Rev, 283*(1), 213-231.
690 doi:10.1111/imr.12655
691 Sauce, D., Larsen, M., Fastenackels, S., Roux, A., Gorochov, G., Katlama, C., . . . Appay, V. (2012).
692 Lymphopenia-driven homeostatic regulation of naive T cells in elderly and
693 thymectomized young adults. *J Immunol, 189*(12), 5541-5548.
694 doi:10.4049/jimmunol.1201235
695 Surh, C. D., & Sprent, J. (2005). Regulation of mature T cell homeostasis. *Semin Immunol, 17*(3),
696 183-191. doi:10.1016/j.smim.2005.02.007
697 Takahashi, H. K., Cambiaghi, T. D., Luchessi, A. D., Hirabara, S. M., Vinolo, M. A., Newsholme, P.,
698 & Curi, R. (2012). Activation of survival and apoptotic signaling pathways in lymphocytes
699 exposed to palmitic acid. *J Cell Physiol, 227*(1), 339-350. doi:10.1002/jcp.22740
700 Tan, H., Yang, K., Li, Y., Shaw, T. I., Wang, Y., Blanco, D. B., . . . Chi, H. (2017). Integrative
701 Proteomics and Phosphoproteomics Profiling Reveals Dynamic Signaling Networks and
702 Bioenergetics Pathways Underlying T Cell Activation. *Immunity, 46*(3), 488-503.
703 doi:10.1016/j.immuni.2017.02.010
704 Tan, J. T., Dudl, E., LeRoy, E., Murray, R., Sprent, J., Weinberg, K. I., & Surh, C. D. (2001). IL-7 is
705 critical for homeostatic proliferation and survival of naive T cells. *Proc Natl Acad Sci U S*
706 *A, 98*(15), 8732-8737. doi:10.1073/pnas.161126098
707 Toth, M. J., & Tchernof, A. (2000). Lipid metabolism in the elderly. *Eur J Clin Nutr, 54 Suppl 3*,
708 S121-125.
709 Ventura, M. T., Casciaro, M., Gangemi, S., & Buquicchio, R. (2017). Immunosenescence in aging:
710 between immune cells depletion and cytokines up-regulation. *Clin Mol Allergy, 15*, 21.
711 doi:10.1186/s12948-017-0077-0
712 Wertheimer, A. M., Bennett, M. S., Park, B., Uhrlaub, J. L., Martinez, C., Pulko, V., . . . Nikolich-
713 Zugich, J. (2014). Aging and cytomegalovirus infection differentially and jointly affect
714 distinct circulating T cell subsets in humans. *J Immunol, 192*(5), 2143-2155.
715 doi:10.4049/jimmunol.1301721
716 Whang, M. I., Tavares, R. M., Benjamin, D. I., Kattah, M. G., Advincula, R., Nomura, D. K., . . . Ma,
717 A. (2017). The Ubiquitin Binding Protein TAX1BP1 Mediates Autophagasome Induction
718 and the Metabolic Transition of Activated T Cells. *Immunity, 46*(3), 405-420.
719 doi:10.1016/j.immuni.2017.02.018
720 Zhang, L., & Romero, P. (2018). Metabolic Control of CD8(+) T Cell Fate Decisions and Antitumor
721 Immunity. *Trends Mol Med, 24*(1), 30-48. doi:10.1016/j.molmed.2017.11.005
722 Zhang, Y., Kurupati, R., Liu, L., Zhou, X. Y., Zhang, G., Hudaihed, A., . . . Ertl, H. C. J. (2017).
723 Enhancing CD8+ T Cell Fatty Acid Catabolism within a Metabolically Challenging Tumor
724 Microenvironment Increases the Efficacy of Melanoma Immunotherapy. *Cancer Cell,*
725 *32*(3), 377-391 e379. doi:10.1016/j.ccell.2017.08.004
726 Zhang, Z., Rahme, G. J., Chatterjee, P. D., Havrda, M. C., & Israel, M. A. (2017). ID2 promotes
727 survival of glioblastoma cells during metabolic stress by regulating mitochondrial
728 function. *Cell Death Dis, 8*(2), e2615. doi:10.1038/cddis.2017.14

729 Zurier, R. B., Rossetti, R. G., Seiler, C. M., & Laposata, M. (1999). Human peripheral blood T
730 lymphocyte proliferation after activation of the T cell receptor: effects of unsaturated
731 fatty acids. *Prostaglandins Leukot Essent Fatty Acids, 60*(5-6), 371-375.
732

733

734 **SUPPLEMENTAL INFORMATION**

735

736

737 **Table S1. Antibodies used in flow cytometry experiments.**
738
739

| ANTIBODY | FLUOROCHROME | SUPPLIER AND REFERENCE |
|---|---|---|
| **Active caspase-3** | PE | BD Biosciences - 561011 |
| **CCR7** | BV650 | BD Biosciences - 563407 |
| **CCR7** | PE-Cy7 | BD Biosciences - 557648 |
| **CD3** | BV605 | BD Biosciences - 563219 |
| **CD8** | APC | BD Biosciences - 555369 |
| **CD8** | APC-Cy7 | BD Biosciences - 557834 |
| **CD8** | FITC | BD Biosciences - 555366 |
| **CD27** | AF700 | BioLegend - 302814 |
| **CD27** | BUV395 | BD Biosciences - 563815 |
| **CD27** | PE | BD Biosciences - 555441 |
| **CD45RA** | ECD | Beckman Coulter - IM2711U |
| **CD45RA** | PerCP-Cy5.5 | eBioscience - 45-0458-42 |
| **CD45RA** | V450 | BD Biosciences - 560362 |
| **CD49d** | PE-Cy7 | BioLegend - 304314 |
| **CD57** | Pacific Blue | BioLegend - 322316 |
| **CD69** | FITC | BD Biosciences - 347823 |
| **CD95** | FITC | BD Biosciences - 555673 |
| **CD134** | BV711 | BD Biosciences - 563664 |
| **pS6** | Pacific Blue | Cell Signaling Technology - 8520S |
| **T-bet** | eFluor660 | eBioscience - 50-5825-80 |

740

741

742

743

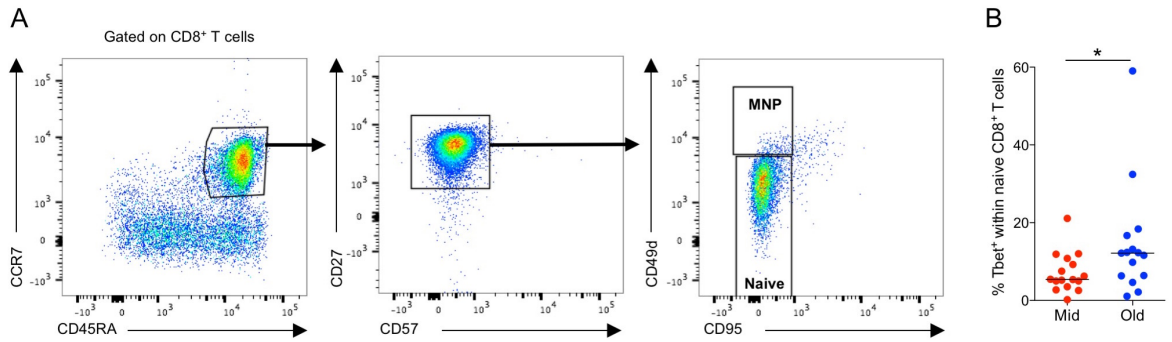


744

745 **Figure S1. T-bet expression in naive CD8$^+$ T cells.** (**A**) Flow cytometric gating strategy used to
746 exclude memory CD8$^+$ T cells with a naive phenotype (MNP). (B) T-bet expression in naive
747 CD8$^+$ T cells (CD3$^+$ CD8$^+$ CD27$^+$ CD45RA$^+$ CCR7$^+$ CD49d$^-$ CD57$^-$ CD95$^-$) from middle-aged
748 (Mid) and elderly individuals (Old). Each dot represents one donor. Horizontal lines indicate
749 median values. * $p < 0.05$ (Mann-Whitney *U* test).

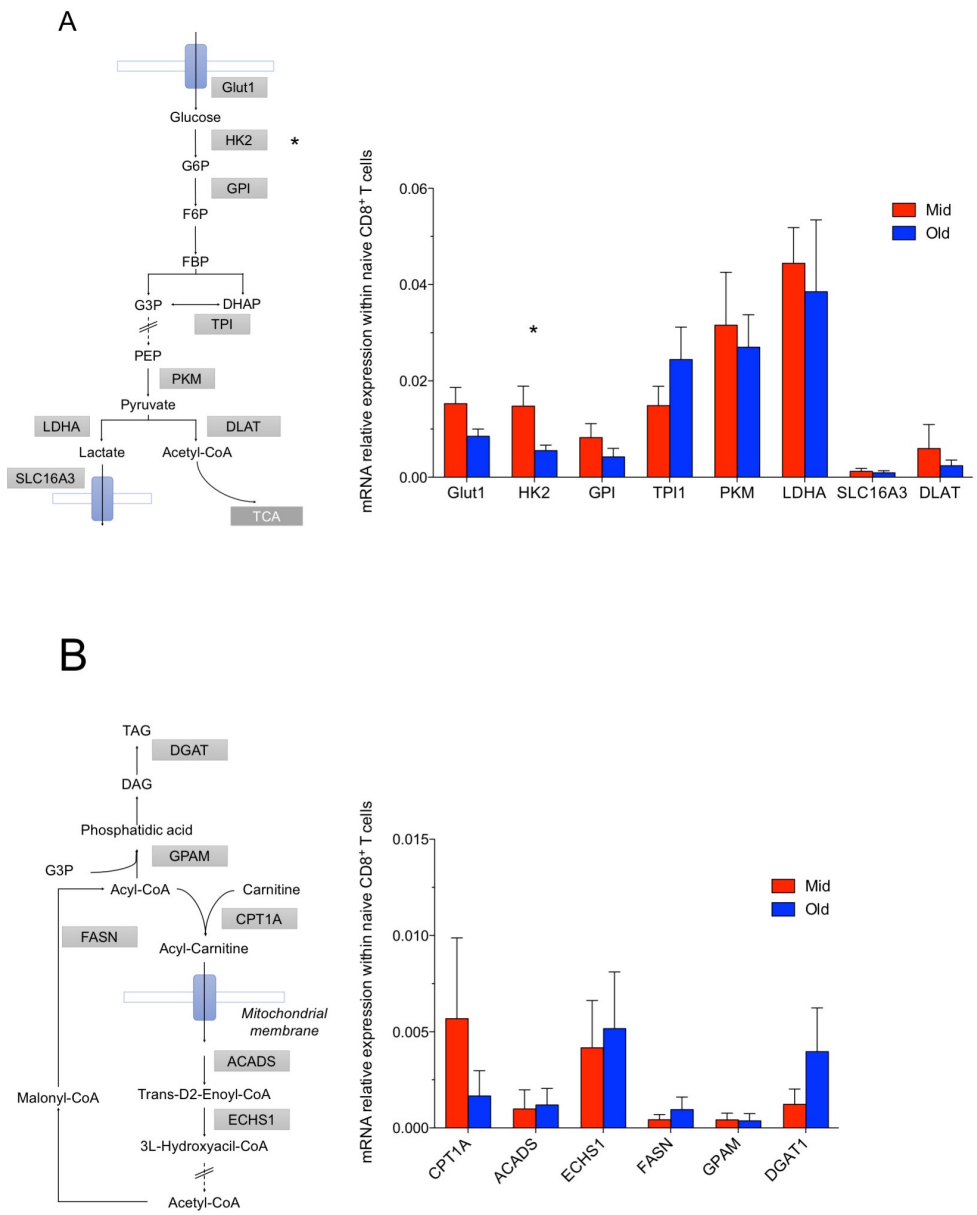


750

751 **Figure S2. Expression of metabolism-related genes in naive CD8$^+$ T cells.** (**A** & **B**) Expression
752 levels of genes related to glucose (A) and fatty acid metabolism (B) were measured in
753 unstimulated naive CD8$^+$ T cells flow-sorted from middle-aged (n = 5; Mid) and elderly
754 individuals (n = 5; Old). Bars indicate mean ± SEM. * $p < 0.05$ (Mann-Whitney *U* test).

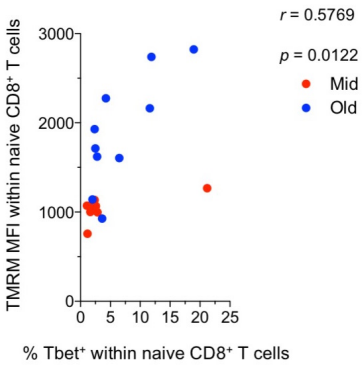


755

756 **Figure S3. Correlation between T-bet expression and mitochondrial membrane potential in**
757 **naive CD8$^+$ T cells.** Correlation between the frequency of unstimulated naive CD8$^+$ T cells that
758 expressed T-bet and basal mitochondrial membrane potential, measured by determining the mean
759 fluorescence intensity (MFI) of TMRM. Each dot represents one donor. Significance was
760 determined using Spearman's rank correlation.

761

762

763

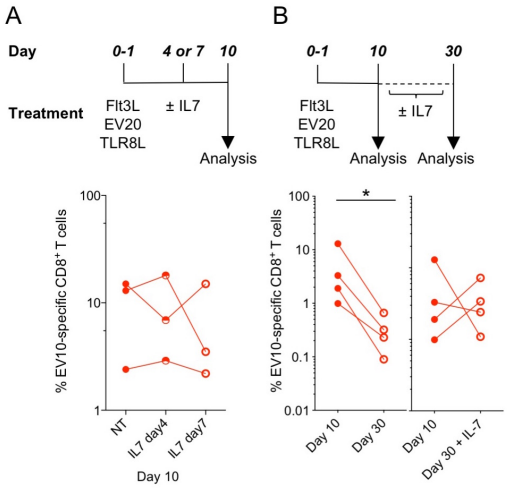


764

765 **Figure S4. Effect of IL-7 on primed epitope-specific CD8$^+$ T cells.** (**A** & **B**) EV10-specific

766 CD8$^+$ T cells were primed and expanded for 10 days in the presence of Flt3 ligand and TLR8L.

767 (A) Cells were left unmanipulated or treated with IL-7 on day 4 or day 7 and tetramer-stained on

768 day 10. Each dot represents one donor. (B) Cells were left unmanipulated or treated with IL-7

769 from day 11 to day 30 and tetramer-stained on day 30. Each dot represents one donor. * $p < 0.05$

770 (Wilcoxon signed rank test). NT: not treated.

771

772

773

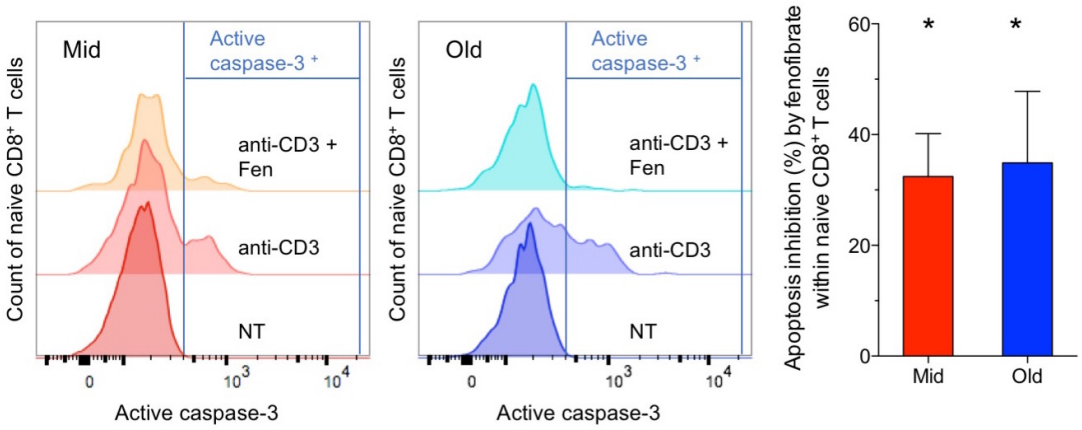


774

775 **Figure S5. Effects of fenofibrate on naive CD8$^+$ T cells.** PBMCs from middle-aged (n = 9; Mid)
776 and elderly individuals (n = 8; Old) were stimulated with plate-bound anti-CD3 in the absence or
777 presence of fenofibrate (Fen). Active caspase-3 expression was measured after 24 hr. Data are
778 shown for naive CD8$^+$ T cells. Left panel: representative flow cytometry profiles. Right panel:
779 data summary. Bars indicate mean ± SEM. * $p < 0.05$ (Wilcoxon signed rank test).

780
781